Effect of Partial Shading on the Performance of Various 4×4 PV Array Configurations

Dharani Kumar Narne[1,2†], **T. A. Ramesh Kumar**[1], and **Rama Koteswara Rao Alla**[2], Non-members

ABSTRACT

Electrical energy usage has drastically increased in recent decades, resulting in significant demand for renewable energy sources, especially solar. With the development of technology, extracting energy from photovoltaic (PV) modules has become easier and more economical. The performance of PV array decreases under an intermittent environment such as partial shading conditions (PSCs), causing fluctuations in PV array power output. This paper presents the analysis of a 4×4 PV array configuration under different PSCs. The power output of PV array depends on factors such as the type of configuration, size of array, and shading patterns. The performance of various types of 4×4 PV array configurations under different shading situations are compared and analyzed in this study, and the results presented.

Keywords: Maximum Power, Partial Shading, PV Array Configurations, Total-Cross-Tied

1. INTRODUCTION

Due to rapid population growth, energy consumption has changed drastically in recent decades. Furthermore, the depletion of fossil fuels and the rise in environmental hazards have drawn more attention to the use of renewable energy to meet global demand [1]. Solar energy plays a key role in the future of clean energy. The entire world's consumption for a year can be served from the solar energy received on the earth's surface in one and half hours. Therefore, solar energy has become an essential element in the sustainable energy system. The cumulative installed capacity of PV is increasing at a very fast rate throughout the world.

Despite the COVID-19 pandemic, total solar energy investment has risen by 12% to USD 148.6 billion. Over 135 GW of new solar PV electricity generation was installed in 2020 worldwide [2], and the 1 TW solar energy capacity barrier is likely to be broken in 2022. A PV system is made up of several elements, such as PV panels that collect sunlight and convert it into electricity. Due to the development of photovoltaic energy, the price of photovoltaic systems has dropped rapidly since their inception [3, 4].

The output of a PV system can be increased either by following the sun's path and positioning the PV panel in such a way that it receives the highest solar radiation or through electrically tracking the point at which the maximum amount of power can be drawn under the conditions of variable insolation and temperature. The total performance of a PV cell varies with changes in temperature and irradiance. Not only does irradiance and temperature affect solar cell efficiency, but also the fill factor [5]. Irradiance and temperature are the key factors in obtaining total power output from PV systems.

Maximum power point tracking (MPPT) techniques are commonly used in PV systems. Many MPPT methods, such as incremental conductance (INC) [6] and perturb and observe (P&O) [7], can be used when constant irradiance is provided throughout the whole PV string. These methods can accurately track the maximum power point (MPP) because there is only one MPP. However, due to interference from clouds, trees, or other objects, some portions of the PV string receive less irradiance under partial shading, resulting in changes in PV output. These traditional MPPT approaches are unable to distinguish global MPP (GMPP) from local MPP (LMPP). Advanced techniques like AI-based and hybrid MPPT [8] are reported in the literature to mitigate these problems.

PV modules can usually be joined in series, parallel, and series-parallel configurations to generate the required power from a PV array. The disadvantage of a series (S) linked PV array is obtaining more than one peak point. The PV array linked in parallel (P) has the benefit of avoiding several peaks but will generate a large quantity of current, resulting in significant voltage dips in the system. The benefits of the series-parallel (SP) PV array outweigh the disadvantages of the S and P linked PV arrays. To obtain the maximum global power from the PV array, the SP PV array is configured as a Bridge-Link (BL), Honey-Comb (HC), and Total-Cross-Tied (TCT) by joining the strings with cross-ties.

To maximize the PV array power under shading situ-

Manuscript received on January 14, 2022; revised on March 10, 2022; accepted on June 21, 2022. This paper was recommended by Associate Editor Kaan Kerdchuen.

[1]The authors are with the Department of Electrical Engineering, Annamalai University, Annamalai Nagar, Chidambaram, Tamilnadu-608002 India.

[2]The authors are with the Department of Electrical and Electronics Engineering, R.V.R. & J.C. College of Engineering, Guntur, Andhra Pradesh-522019, India.

[†]Corresponding author: dharaninarne@gmail.com

Digital Object Identifier: 10.37936/ecti-eec.2022203.247518

ations, dynamic [9] and static reconfiguration methods are employed. If the modules are rearranged at the time of installation, only then can such configurations be called static. If an algorithm is used for reconfiguration or sensors employed for automatic switching, then this type of reconfiguration is known as dynamic. Optimal Sudoku [10], Sudoku [11], Zigzag [12] pattern, and modified Sudoku [13], etc., have been recently suggested for enhancing the PV array power. Various types of interchanging connections for dynamic PV arrays have been proposed for non-uniform irradiance situations using irradiance evolution [14], genetic algorithms [15], and PSO [16] in the literature.

To extract maximum power from a PV array, the selection of a proper configuration [17] and materials [18] are very important. This paper presents an analysis of the 4×4 PV array connected in S, P, SP, BL, HC, and TCT PV array configurations under long narrow (LN), long wide (LW), short narrow (SN), short wide (SW), and uniform (UN) shading patterns. The main drawback of the series PV array configuration is its high output voltage and low output current, whereas the parallel PV array configuration has a low output voltage and high output current [19, 20]. Hence, the series and parallel PV array topologies are not preferable for practical implementation.

Other PV array configurations such as SP, TCT, BL, and HC are preferred for practical implementation since they provide the required output voltage and current [21–23]. The limitations of the S-P PV array configuration are its greater multi-peak effect and low maximum power in most cases when compared to cross-tied configurations. The limitations of the TCT PV array configuration are its high redundancy, high wiring loss, numerous connections, poor performance during row-wise shading conditions, and the requirement for an unrealistic number of switches and sensors for reconfiguration [24]. The B-L PV array configuration limitations are its high redundancy, higher wiring loss, and lower maximum power than TCT during partial shading. Whereas the HC configuration limitations are that it has slightly lower maximum power than the TCT in most cases, higher wiring loss, and higher redundancy [25, 26]. Therefore, it is essential to analyze the best performing PV array configuration under various partial shading conditions to choose the optimal PV array for industrial applications and power delivery to the respective loads.

The remaining part of this paper is framed as follows: Section 2 presents the various PV array configurations used. Section 3 discusses the performance measures and various shading conditions, Section 4 describes the simulation results and provides a discussion, while the conclusions are given in Section 5.

2. PV ARRAY CONFIGURATIONS

Multiple solar modules can be linked in series to make a photovoltaic string in order to produce the necessary voltage and power output in a photovoltaic system. These solar strings may be joined in parallel (P) to make a photovoltaic array for power enhancement [27, 28]. These modules can only be linked in series since the output voltage will be excessively high, making them unsuitable for grid-connected inverters and energy storage. As a result, both parallel and series connections are used to link these solar modules.

In the simple series string shown in Fig. 1(a), to protect the PV module from reverse breakdown, each PV module is joined with a bypass diode [29]. The main purpose of this diode is that when a module is less illuminated than the others, it is eliminated and compared to one which is more illuminated to allow the flow of higher currents. The same also happens in the case of parallel configuration. The drawback of parallel configuration is its terminal voltage is very low and needs boosting before linking to the grid with the help of an inverter. Therefore, parallel configuration is appropriate for achieving higher voltage boost ratios.

The series-parallel (SP) connected PV array configuration is shown in Fig. 1(c). This SP topology [30] has a few benefits, such as easy implementation and no redundant connection leads, making it cost-effective. With the SP configuration, the required current and voltage can be achieved [31]. Since there is no interconnection among strings in a series, if any module is less illuminated, the corresponding diode will then be on, and the respective string voltage drop occurs. In such a case, the remaining modules of a similar string are exempt from the generation of power since the blocking diode needs to be activated [32].

Fig. 1(d) shows the Bridge-Link configuration. Since the configuration resembles a bridge rectifier circuit, it is known as a BL. A cross-HC link is connected to the two groups of every four neighboring modules so that a brick pattern is achieved as given in [33]. This configuration has more alternative paths for current flow due to it having fewer cross-tie links in comparison to the SP configuration, resulting in fewer mismatch losses [34].

Fig. 1(e) gives the Honey-Comb (HC) configuration. In similarity to the BL configuration, it connects the adjacent series string to form a combined structure in accordance with the header method of bonding suggested in [35].

Fig. 1(f) gives the Total-Cross-Tied (TCT) configuration proposed in [36], which involves cross-tying the rows of the junction. The inclusion of a potential difference in all rows gives the array voltage, while the addition of currents in all strings results in the array current. The cross-ties of this configuration stop the bypass diodes turning unnecessarily, resulting in an increased lifetime for the PV array [37]. This configuration has the advantage of the high current in the more illuminated module flowing in other strings connected in series automatically through cross-ties.

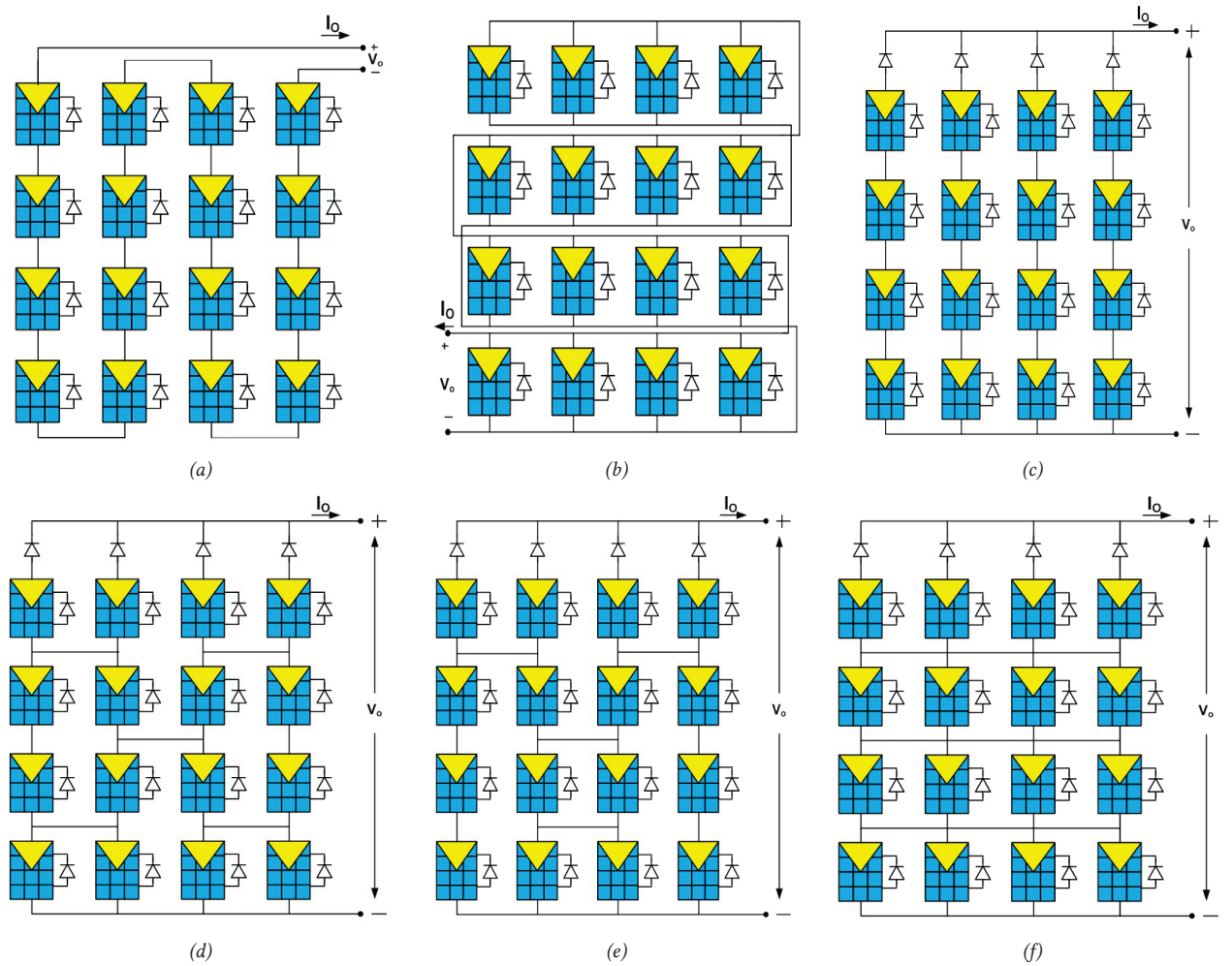

***Fig. 1**: (a) Series, (b) parallel, (c) series-parallel, (d) Bridge-Link, (e) Honey-Comb, and (f) Total-Cross-Tied connected PV arrays.*

3. PERFORMANCE MEASURES AND VARIOUS SHADING CONDITIONS OF PV ARRAYS

The various performance measures and shading patterns considered in this work are described in this section. The measures used for the analysis are efficiency, maximum power (P_{MP}), mismatch power loss (%MPL), and fill factor (FF).

3.1 Maximum Power (P_{MP})

This is the most important measure of the PV array since it provides information on the highest power that can be drawn under a particular situation. In general, the PV characteristic peak point is that at which the highest power can be produced, but because of partial shading, many peak points may occur. The global peak point gives the maximum power extracted from the PV array (P_{GMPP}).

3.2 Mismatch Power Loss (MPL)

Mismatch losses can be evaluated with the help of the following formula,

$$\%\text{MPL} = \frac{P_{sum} - P_{GMPP}}{P_{sum}} \times 100 \tag{1}$$

The percentage of mismatch power loss (MPL) is represented by %MPL, while the sum of total power when the individual modules are joined separately is represented by P_{sum}. If all the modules present in the system deliver their maximum power, then the value of this indicator is one.

3.3 Fill Factor (FF)

It is also important to comment on the performance of the system. This can be obtained from the ratio between global maximum peak power (P_{GMPP}) and the product of V_{OC} (open circuit voltage) and I_{SC} (short circuit current) of the array under a particular shading condition. It can be evaluated from the following expression,

$$\text{FF} = \frac{P_{GMPP}}{I_{SC} \times V_{OC}} \tag{2}$$

To conclude that the array performance is better, the fill factor value should be nearer to one.

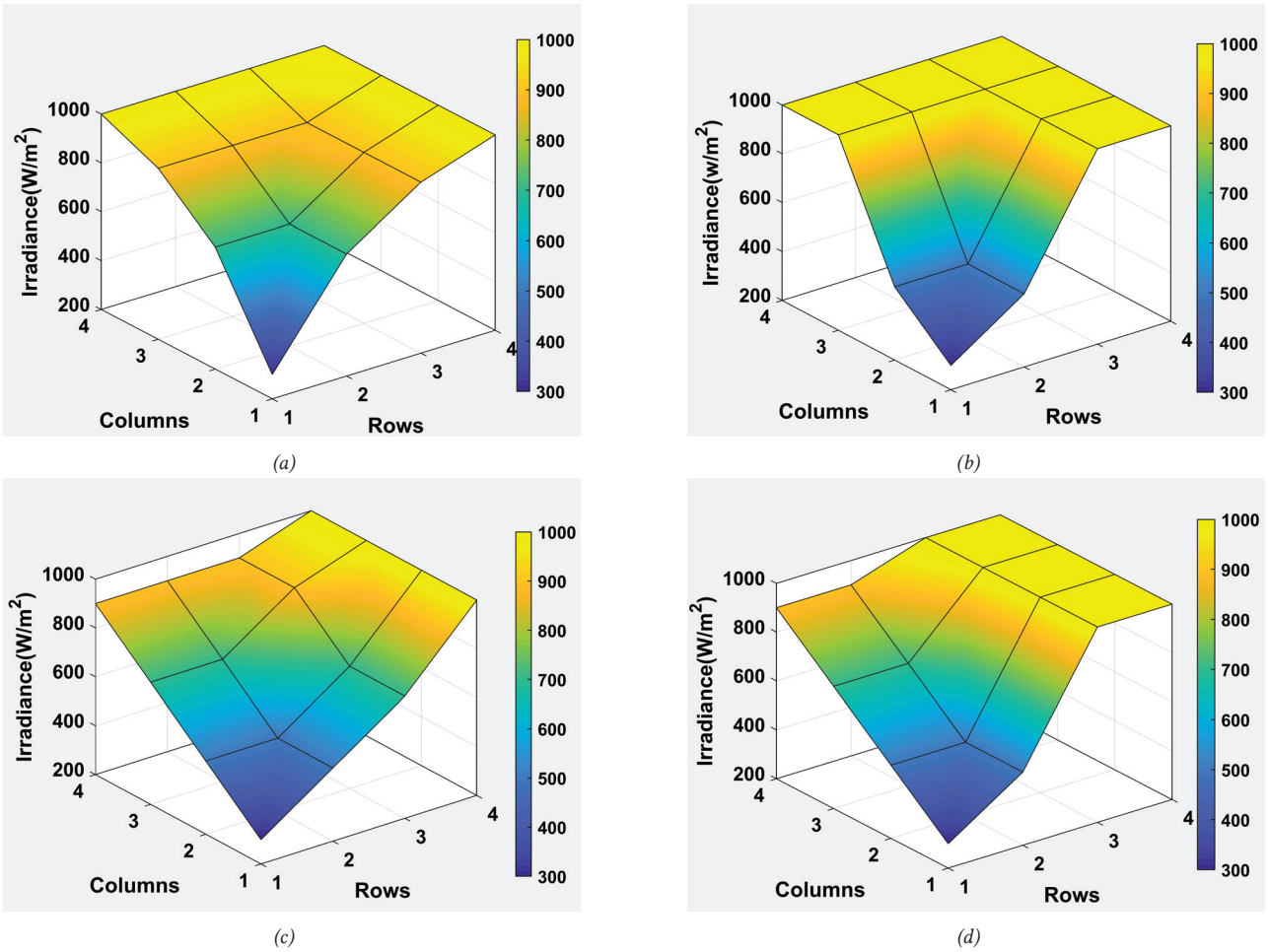

***Fig. 2**: (a) Short wide, (b) short narrow, (c) long wide, and (d) long narrow shading patterns.*

3.4 Efficiency

For comparing the performance of the PV modules, the most commonly used parameter is efficiency. The efficiency of a PV module depends on its temperature, spectrum, and intensity of the incident sunlight. Therefore, efficiency (η) is defined as the ratio between the maximum power obtained and the solar power input to panels.

$$\%\text{Efficiency} = \frac{V_{MP} \times I_{MP}}{I \times A} \times 100 \tag{3}$$

Here, the PV array area is represented by A and the solar irradiance per unit area is given by I.

3.5 Partial Shading Patterns

Various partial shading conditions can occur on the PV system. Some of the most commonly occurring shading patterns considered in this work are short wide (SW), short narrow (SN), long wide (LW), and long narrow (LN). Fig. 2 depicts the irradiance changes in the rows and columns of PV panels of up to 1000 W/m^2.

4. SIMULATION RESULTS AND DISCUSSION

This section presents an analysis of the results obtained from simulation for various 4×4 PV configurations considered under various partial shading conditions.

4.1 Series

The PV array current reduces in the PSC due to low irradiance levels, which leads to nonlinear characteristics in PV modules and mismatch power losses. Consequently, under this condition, modules dissipate power rather than delivering it since shaded modules operate in reverse bias, causing hot spots and leading to damage to the PV modules. Figs. 3(a) and 3(b) show the I-V and P-V curves of a series configuration. Since less cabling is used, this configuration has the advantage of reducing cabling losses. The drawback of this configuration is that it results in significant mismatch loss, leading to a decrease in power generation capability under PSCs.

4.2 Parallel

Corresponding to the isolation level, the current produced from every PV module flows with no limit while the voltage at MPP is constant under PSCs.

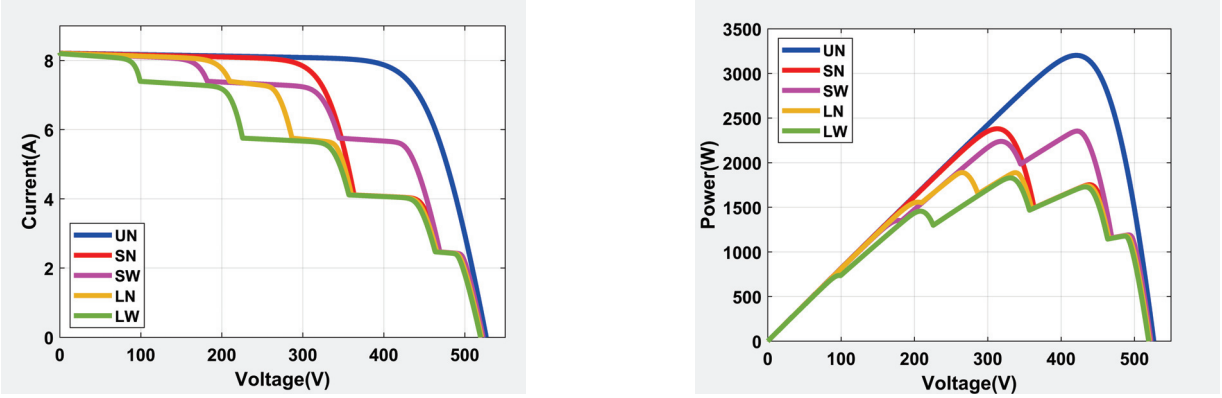

(a) (b)

***Fig. 3**: (a) I-V and (b) P-V curves of a series PV configuration.*

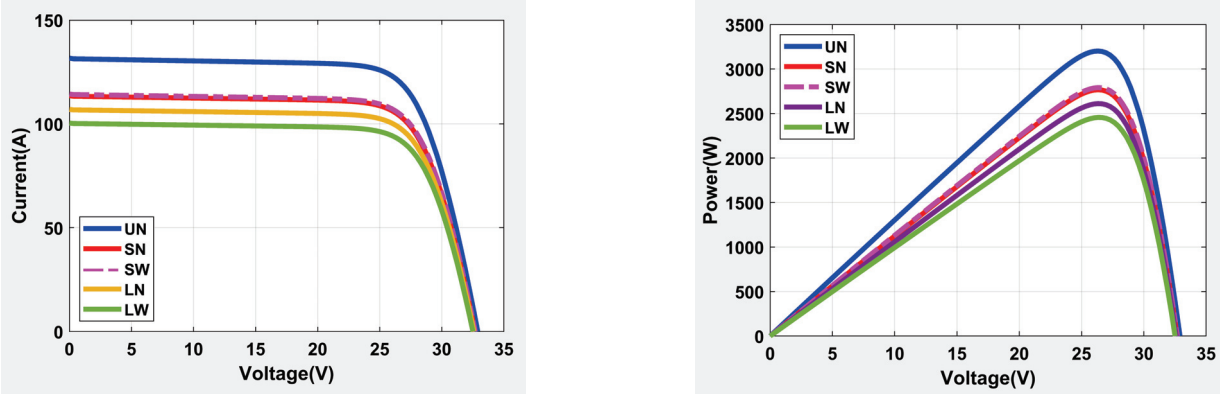

(a) (b)

***Fig. 4**: (a) I-V and (b) P-V curves under parallel PV conditions.*

Therefore, under PSCs, the parallel-connected PV array gives effective results with no multiple MPPs in the P-V characteristics. This configuration produces more power than a series connection because of the high current and low voltage at the terminal. However, the occurrence of significant power loss and voltage drop is due to high currents. The I-V and P-V curves for the parallel-connected PV configuration under various shadings are shown in Figs. 4(a) and 4(b).

4.3 Uniform

Under uniform irradiance conditions, the considered 4×4 PV array configuration I-V and P-V curves are given in Figs. 5(a) and 5(b). The performance of the configuration in terms of various measures is shown in Table 1.

From the results in Table 1, it can be observed that the maximum power is extracted by the parallel configuration of 3202.258 W. The SP, BL, HC, and TCT configurations give 3180.611 W. There are zero mismatch power losses in all cases. The efficiency of the P configuration is also compared to other configurations.

4.4 Short narrow

Figs. 6(a) and 6(b) give the I-V and P-V curves of the SP, BL, HC, and TCT configurations under SN shading conditions. Table 2 presents the results of the measures under SN shading conditions.

As can be observed, the maximum power is obtained in the parallel configuration case, followed by TCT. The MPL also generates less power than the parallel case, followed by TCT. The fill factor is 74.064 for P, 56.502 for TCT, and 52.736 for SP configurations. The parallel configuration is shown to be the most efficient at 12.25%, followed by TCT with 10.787%.

4.5 Short wide

The I-V and P-V curves of SP, BL, HC, and TCT under SW conditions are presented in Figs. 7(a) and 7(b). The parameters evaluated for this shading situation are listed in Table 3.

As can be observed from Table 3, under SW conditions, the efficiency, fill factor, and maximum power are high in the case of the parallel configuration, while TCT once again takes second position in this shading pattern. The MPL is high in the case of series configuration and extracting the least power.

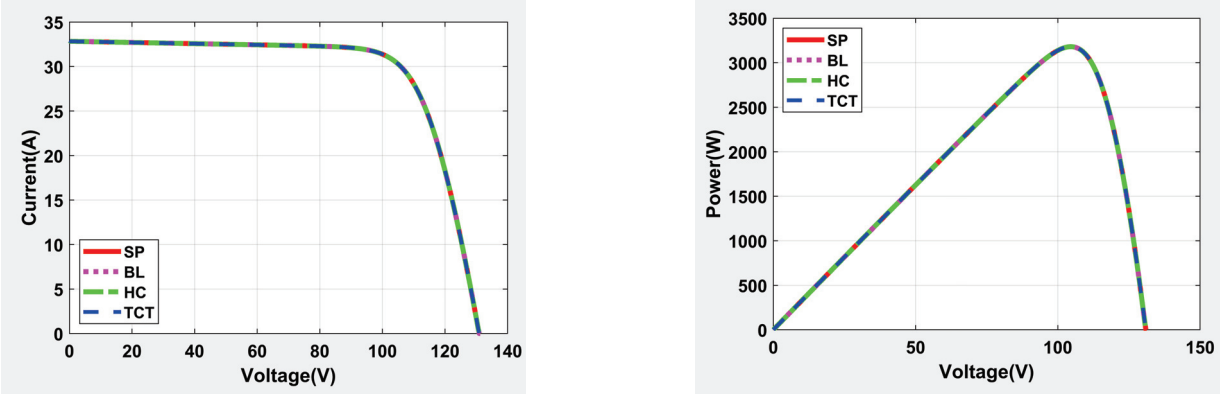

(a) (b)

***Fig. 5**: (a) I-V and (b) P-V curves uniform irradiance conditions.*

***Table 1**: Results of various measures under uniform irradiance conditions.*

	V_{OC}	I_{SC}	V_{MP}	I_{MP}	P_{MP}	MPL	FF	Efficiency
S	526.400	8.228	420.791	7.610	3202.172	0.000	73.934	14.186
P	32.900	131.646	26.320	121.666	3202.258	0.000	73.936	14.187
SP	130.942	32.911	104.622	30.401	3180.611	0.000	73.805	14.091
BL	130.942	32.911	104.622	30.401	3180.611	0.000	73.805	14.091
HC	130.942	32.911	104.622	30.401	3180.611	0.000	73.805	14.091
TCT	130.942	32.911	104.622	30.401	3180.611	0.000	73.805	14.091

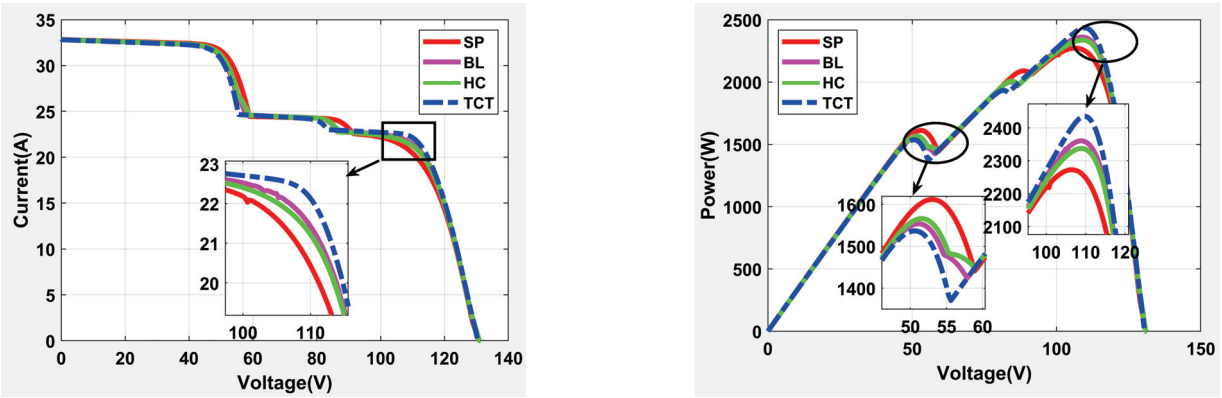

(a) (b)

***Fig. 6**: (a) I-V and (b) P-V curves under short narrow conditions.*

***Table 2**: Results of various measures under short narrow conditions.*

	V_{OC}	I_{SC}	V_{MP}	I_{MP}	P_{MP}	MPL	FF	Efficiency
S	522.123	8.228	312.879	7.607	2380.206	25.669	55.406	10.545
P	32.900	113.544	26.320	105.119	2766.744	13.598	74.064	12.257
SP	130.942	32.911	106.596	21.320	2272.617	28.356	52.736	10.068
BL	130.942	32.910	108.899	21.676	2360.472	25.612	54.776	10.458
HC	130.942	32.910	108.899	21.463	2337.313	26.335	54.238	10.355
TCT	130.942	32.910	109.886	22.158	2434.846	23.289	56.502	10.787

4.6 Long narrow

Figs. 8(a) and 8(b) give the *I-V* and *P-V* curves of SP, BL, HC, ad TCT configurations under LN shading conditions. Table 4 presents the results of various measures.

As can be observed from Table 4, the maximum power

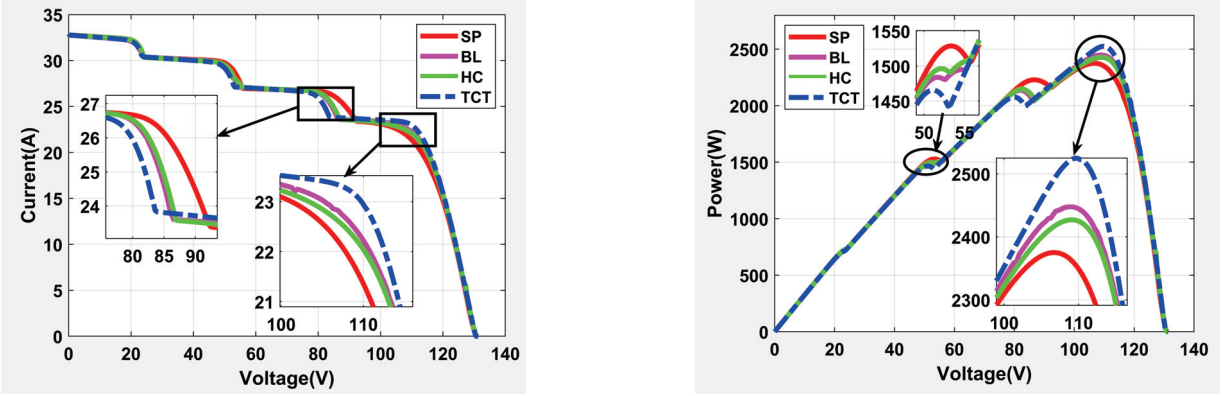

(a) (b)

***Fig. 7**: (a) I-V and (b) P-V curves under short wide conditions.*

***Table 3**: Results of various measures under short wide conditions.*

	V_{OC}	I_{SC}	V_{MP}	I_{MP}	P_{MP}	MPL	FF	Efficiency
S	522.781	8.228	421.778	5.581	2354.058	26.486	54.730	10.429
P	32.900	114.367	26.320	106.056	2791.407	12.828	74.187	12.367
SP	130.942	32.909	106.596	22.281	2375.052	25.157	55.117	10.522
BL	130.942	32.908	108.899	22.478	2447.828	22.884	56.807	10.845
HC	130.942	32.908	109.228	22.220	2427.023	23.534	56.323	10.752
TCT	130.613	32.908	109.557	23.045	2524.775	20.481	58.741	11.185

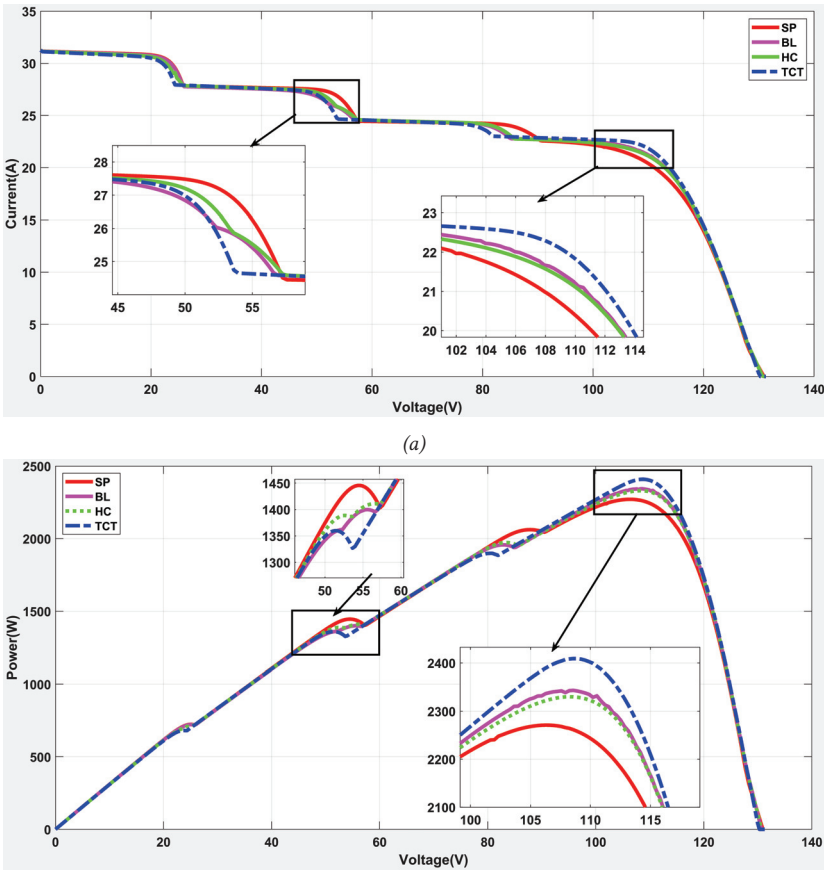

(a)

(b)

***Fig. 8**: (a) I-V and (b) P-V curves under long narrow conditions.*

***Table 4**: Results of various measures under long narrow conditions.*

	V_{OC}	I_{SC}	V_{MP}	I_{MP}	P_{MP}	MPL	FF	Efficiency
S	520.807	8.228	265.174	7.124	1889.007	41.009	44.084	8.369
P	32.900	106.962	26.320	99.220	2611.458	18.447	74.209	11.569
SP	130.942	31.264	106.267	21.371	2270.992	28.406	55.475	10.061
BL	130.942	31.263	108.570	21.585	2343.438	26.144	57.245	10.382
HC	130.942	31.263	108.241	21.527	2330.102	26.560	56.920	10.323
TCT	130.284	31.262	108.570	22.188	2408.943	24.098	59.145	10.672

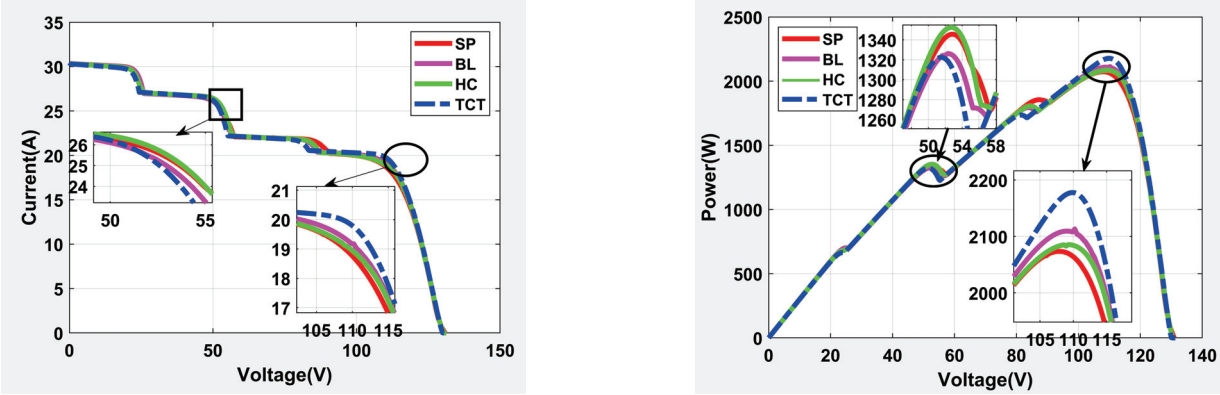

(a) *(b)*

***Fig. 9**: (a) I-V and (b) P-V curves under long wide conditions.*

***Table 5**: Results of various measures under long wide conditions.*

	V_{OC}	I_{SC}	V_{MP}	I_{MP}	P_{MP}	MPL	FF	Efficiency
S	519.491	8.227	330.645	5.533	1829.339	42.872	42.802	8.104
P	32.571	100.380	26.320	93.320	2456.172	23.297	75.124	10.881
SP	130.942	30.441	107.912	19.215	2073.528	34.573	52.021	9.186
BL	130.613	30.441	110.215	19.173	2113.154	33.335	53.148	9.362
HC	130.613	30.440	109.228	19.093	2085.543	34.198	52.455	9.240
TCT	130.284	30.439	109.886	19.819	2177.798	31.317	54.915	9.648

2611.458 W is obtained by the parallel configuration, while the least power is extracted from the series configuration. The MPL equates to 18.447 for P, 28.406 for SP, 41.009 for S, 26.144 for BL, 26.56 for HC, and 24.098 for TCT can be noticed. The efficiency is high for the parallel and low for the series configuration. In the case of FF, P has 74.209, S has 44.084, SP has 55.475, BL has 57.24, HC has 56.9, and TCT has 59.145.

4.7 Long wide

In long wide shading conditions, the characteristics of 4×4 SP, BL, HC, and TCT in terms of I-V and P-V are shown in Figs. 9(a) and 9(b). The calculated measures of SP, BL, HC, and TCT under LW shading conditions are presented in Table 5.

As can be observed from the results, the S configuration exhibits the least power extraction of 1829.339 W, while the highest power extraction is obtained from the P configuration with 2456.172 W. The TCT has 2177.798 W, SP has 2073.528 W, BL has 2113.154 W, and the HC has 2085.543 W. In terms of MPL, P has 23.297, TCT has 31.317, BL has 33.335, HC has 34.198, SP has 34.573, and S has 42.872. The same type of ranking can be observed for efficiency and FF. The parallel configuration gives efficient results but has the drawback of less terminal voltage.

5. CONCLUSION

This paper examines the performance of 4×4 PV array configurations: S, P, SP, BL, HC, and TCT in the presence of various PSCs. The PSCs considered are SW, SN, LW, LN, and uniform shadings. The results of the considered configurations for various shading patterns are examined using measures such as V_{OC}, I_{SC}, V_{MP}, I_{MP}, P_{MP}, MPL, and FF. The output characteristics of these configurations are described for various shading conditions. The results obtained indicated that the highest power extraction is from the P configuration, followed by TCT, SP, BL, and

HC. However, due to the P configuration exhibiting less terminal voltage, the next best TCT configuration is preferred under various PSCs. From the results, it can be concluded that the performance of the TCT PV array configuration is superior to the other configurations. The considered TCT array topology has few multi-peak effects, a smooth inflection point, higher maximum power in most cases, long operational lifetime, good fault tolerance, and low variation intervals in MPP voltage during partial shading while responding and adapting well to random shading patterns. Hence, the TCT PV array configuration can be recommended for most industrial applications.

ACKNOWLEDGMENTS

The authors gratefully acknowledge the support provided by ILIOS Power Private Limited Hyderabad, India under an industry-sponsored research project for this work.

REFERENCES

[1] A. M. Omer, "Energy, environment and sustainable development," *Renewable and Sustainable Energy Reviews*, vol. 12, no. 9, pp. 2265–2300, Dec. 2008.

[2] A. Jäger-Waldau, "Snapshot of photovoltaics - March 2021," *EPJ Photovoltaics*, vol. 12, 2021, Art. no. 2.

[3] N. A. Lee, G. E. Gilligan, and J. Rochford, "Solar energy conversion," in *Green Chemistry: An Inclusive Approach*, B. Török and T. Dransfield, Eds. Amsterdam, The Netherlands: Elsevier, 2018, pp. 881–918.

[4] S. Jiang, C. Wan, C. Chen, E. Cao, and Y. Song, "Distributed photovoltaic generation in the electricity market: status, mode and strategy," *CSEE Journal of Power and Energy Systems*, vol. 4, no. 3, pp. 263–272, Sep. 2018.

[5] P. Manganiello, M. Balato, and M. Vitelli, "A survey on mismatching and aging of PV modules: The closed loop," *IEEE Transactions on Industrial Electronics*, vol. 62, no. 11, pp. 7276–7286, Nov. 2015.

[6] L. Shengqing, L. Fujun, Z. Jian, C. Wen, and Z. Donghui, "An improved MPPT control strategy based on incremental conductance method," *Soft Computing*, vol. 24, pp. 6039–6046, Apr. 2020.

[7] S.-C. Wang, H.-Y. Pai, G.-J. Chen, and Y.-H. Liu, "A fast and efficient maximum power tracking combining simplified state estimation with adaptive perturb and observe," *IEEE Access*, vol. 8, pp. 155 319–155 328, 2020.

[8] D. D. Martínez, R. T. Codorniu, R. Giral, and L. V. Seisdedos, "Evaluation of particle swarm optimization techniques applied to maximum power point tracking in photovoltaic systems," *International Journal of Circuit Theory and Applications*, vol. 49, no. 7, pp. 1849–1867, Jul. 2021.

[9] B. K. Karmakar and G. Karmakar, "A current supported PV array reconfiguration technique to mitigate partial shading," *IEEE Transactions on Sustainable Energy*, vol. 12, no. 2, pp. 1449–1460, Apr. 2021.

[10] M. Horoufiany and R. Ghandehari, "Optimization of the Sudoku based reconfiguration technique for PV arrays power enhancement under mutual shading conditions," *Solar Energy*, vol. 159, pp. 1037–1046, Jan. 2018.

[11] G. S. Krishna and T. Moger, "A novel adaptive dynamic photovoltaic reconfiguration system to mitigate mismatch effects," *Renewable and Sustainable Energy Reviews*, vol. 141, May 2021, Art. no. 110754.

[12] S. Vijayalekshmy, G. Bindu, and S. R. Iyer, "A novel Zig-Zag scheme for power enhancement of partially shaded solar arrays," *Solar Energy*, vol. 135, pp. 92–102, Oct. 2016.

[13] K. Rajani and T. Ramesh, "Maximum power enhancement under partial shadings using modified sudoku reconfiguration," *CSEE Journal of Power and Energy Systems*, vol. 7, no. 6, pp. 1187–1201, Nov. 2021.

[14] J. P. Storey, P. R. Wilson, and D. Bagnall, "Improved optimization strategy for irradiance equalization in dynamic photovoltaic arrays," *IEEE Transactions on Power Electronics*, vol. 28, no. 6, pp. 2946–2956, Jun. 2013.

[15] S. N. Deshkar, S. B. Dhale, J. S. Mukherjee, T. S. Babu, and N. Rajasekar, "Solar PV array reconfiguration under partial shading conditions for maximum power extraction using genetic algorithm," *Renewable and Sustainable Energy Reviews*, vol. 43, pp. 102–110, Mar. 2015.

[16] T. S. Babu, J. P. Ram, T. Dragičević, M. Miyatake, F. Blaabjerg, and N. Rajasekar, "Particle swarm optimization based solar PV array reconfiguration of the maximum power extraction under partial shading conditions," *IEEE Transactions on Sustainable Energy*, vol. 9, no. 1, pp. 74–85, Jan. 2018.

[17] T. Ramesh, K. Rajani, and A. K. Panda, "A novel triple-tied-cross-linked PV array configuration with reduced number of cross-ties to extract maximum power under partial shading conditions," *CSEE Journal of Power and Energy Systems*, vol. 7, no. 3, pp. 567–581, May 2021.

[18] S. Vunnam, M. V. Sri, and A. R. K. Rao, "Performance analysis of mono crystalline, poly crystalline and thin film material based 6 × 6 T-C-T PV array under different partial shading situations," *Optik*, vol. 248, Dec. 2021, Art. no. 168055.

[19] S. R. Pendem and S. Mikkili, "Modelling and performance assessment of PV array topologies under partial shading conditions to mitigate the mismatching power losses," *Solar Energy*, vol. 160, pp. 303–321, Jan. 2018.

[20] S. R. Pendem and S. Mikkili, "Modeling, simulation, and performance analysis of PV array configurations (series, series-parallel, bridge-linked, and

honey-comb) to harvest maximum power under various partial shading conditions," *International Journal of Green Energy*, vol. 15, no. 13, pp. 795–812, 2018.

[21] S. Moballegh and J. Jiang, "Modeling, prediction, and experimental validations of power peaks of PV arrays under partial shading conditions," *IEEE Transactions on Sustainable Energy*, vol. 5, no. 1, pp. 293–300, Jan. 2014.

[22] R. Pachauri, R. Singh, A. Gehlot, R. Samakaria, and S. Choudhury, "Experimental analysis to extract maximum power from PV array reconfiguration under partial shading conditions," *Engineering Science and Technology, an International Journal*, vol. 22, no. 1, pp. 109–130, Feb. 2019.

[23] S. Bana and R. Saini, "Experimental investigation on power output of different photovoltaic array configurations under uniform and partial shading scenarios," *Energy*, vol. 127, pp. 438–453, May 2017.

[24] S. R. Pendem, S. Mikkili, S. S. Rangarajan, S. Avv, R. E. Collins, and T. Senjyu, "Optimal hybrid PV array topologies to maximize the power output by reducing the effect of non-uniform operating conditions," *Electronics*, vol. 10, no. 23, 2021, Art. no. 3014.

[25] S. R. Pendem, V. V. Katru, and S. Mikkili, "Hybrid PV array configurations for mitigating the mismatching power loss and number of peaks in the output characteristics under various PSCs," in *IECON 2019 - 45th Annual Conference of the IEEE Industrial Electronics Society*, 2019, pp. 2377–2382.

[26] R. K. Pachauri *et al.*, "Impact of partial shading on various PV array configurations and different modeling approaches: A comprehensive review," *IEEE Access*, vol. 8, pp. 181 375–181 403, 2020.

[27] A. Ali *et al.*, "Investigation of MPPT techniques under uniform and non-uniform solar irradiation condition–a retrospection," *IEEE Access*, vol. 8, pp. 127 368–127 392, 2020.

[28] Y.-C. Liu, M.-C. Chen, C.-Y. Yang, K. Kim, and H.-J. Chiu, "High-efficiency isolated photovoltaic microinverter using wide-band gap switches for standalone and grid-tied applications," *Energies*, vol. 11, no. 3, 2018, Art. no. 569.

[29] A. Dolara, G. C. Lazaroiu, S. Leva, and G. Manzolini, "Experimental investigation of partial shading scenarios on PV (photovoltaic) modules," *Energy*, vol. 55, pp. 466–475, Jun. 2013.

[30] P. S. Rao, G. S. Ilango, and C. Nagamani, "Maximum power from PV arrays using a fixed configuration under different shading conditions," *IEEE Journal of Photovoltaics*, vol. 4, no. 2, pp. 679–686, Mar. 2014.

[31] P. K. Bonthagorla and S. Mikkili, "Performance investigation of hybrid and conventional PV array configurations for grid-connected/standalone PV systems," *CSEE Journal of Power and Energy Systems*, vol. 8, no. 3, pp. 682–695, May 2020.

[32] J. D. Bastidas-Rodriguez, J. M. Cruz-Duarte, and R. Correa, "Mismatched series–parallel photovoltaic generator modeling: An implicit current–voltage approach," *IEEE Journal of Photovoltaics*, vol. 9, no. 3, pp. 768–774, May 2019.

[33] D. P. Winston, S. Kumaravel, B. P. Kumar, and S. Devakirubakaran, "Performance improvement of solar PV array topologies during various partial shading conditions," *Solar Energy*, vol. 196, pp. 228–242, Jan. 2020.

[34] G. Velasco-Quesada, F. Guinjoan-Gispert, R. Pique-Lopez, M. Roman-Lumbreras, and A. Conesa-Roca, "Electrical PV array reconfiguration strategy for energy extraction improvement in grid-connected PV systems," *IEEE Transactions on Industrial Electronics*, vol. 56, no. 11, pp. 4319–4331, Nov. 2009.

[35] M. Jazayeri, S. Uysal, and K. Jazayeri, "A comparative study on different photovoltaic array topologies under partial shading conditions," in *2014 IEEE PES T&D Conference and Exposition*, 2014.

[36] P. Bhatnagar and R. Nema, "Maximum power point tracking control techniques: State-of-the-art in photovoltaic applications," *Renewable and Sustainable Energy Reviews*, vol. 23, pp. 224–241, Jul. 2013.

[37] M. Alonso-García, J. Ruiz, and W. Herrmann, "Computer simulation of shading effects in photovoltaic arrays," *Renewable Energy*, vol. 31, no. 12, pp. 1986–1993, Oct. 2006.

Dharani Kumar Narne received his B.Tech. from Nalanda Institute of Engineering and Technology, Affiliated to A.N.U, Andhra pradesh, India in 2008. He received his M.Tech. degree in Power Systems from R.V.R. & J.C. College of Engineering, affiliated to ANU, India in 2010. He is currently pursuing Ph.D. degree (Part Time) with Annamalai University, Chidambram, India. Currently, he is working as Assistant Professor in R.V.R. & J.C. College of Engineering, Guntur, Andhra Pradesh, India. His area of interests includes Power Systems, Renewable Energy, power generation, power grids, power supply quality, power transmission reliability, etc.

T. A. Ramesh Kumar received his B.Eng. in Electrical and Electronics Engineering in 2002. He received his M.Eng. in Power System Engineering in 2008, and the Ph.D. in Electrical Engineering from Annamalai University, Tamilnadu, India, in 2013. He is working as Associate Professor in the Department of Electrical Engineering, Annamalai University, Tamilnadu, India. His research interests are Power Systems, Control Systems, and Electrical Measurements.

Rama Koteswara Rao Alla received his B.Tech. (Electrical and Electronics Engineering) in 2008 from Loyola Institute of Technology and Management, Guntur, Affiliated to JNTU Hyderabad, India, M.Tech. (Control Systems) in 2010 and Ph.D. from Electrical Engineering Department, National Institute of Technology Kurukshetra, Haryana, India, in October 2017. Currently, he is working as Associate Professor in R.V.R. & J.C. College of Engineering, Guntur, Andhra Pradesh, India. His area of interests includes Control Systems, Solar PV Systems, Stability Analysis of Time Delay Systems, and Reliability Engineering.